Functionalized Boron Nitride Nanotubes and Their Polymer Nanocomposites

J. W. Guan[*], A. Derdouri[**], B. Ashrafi[***], A. Benhalima[**], K. S. Kim[*], C. T. Kingston[*] and B. Simard[*]

[*]Security and Disruptive Technologies Research Centre, NRC, 100 Sussex Dr., Ottawa, K1A 0R6, Canada, jingwen.guan@nrc-cnrc-gc.ca
[**]Automotive and Surface Transportation Research Centre, NRC, Boucherville, QC, J4B 6Y4, Canada, abdelkader.benhalima@nrc-cnrc.gc.ca
[***]Aerospace Research Centre, NRC, Montreal, QC, H3T 2B2, Canada behnam.ashrafi@nrc-cnrc.gc.ca

ABSTRACT

Carbon nanotubes (CNTs) integrated polymer nanocomposites demonstrated promising trends to repalce traditional metal materials for lightweighting application. Similarly, boron nitride nanotubes (BNNTs), which are structurally analogous to CNTs, possess complimentary properties that create new possibilities in the fields of structural and functional composites, particularly in the fabrication of optically transparent, thermally and scratch resistant materials. Just like with CNTs, the main issues in manufacturing nanocomposites with superlative properties are dispersion and interfacial adhesion with a polymer matrix. The most effective method used to resolve these issues is surface chemical functionalizations to obtain stronger adhesion at the interface of BNNT and the polymer. In this paper, we report the chemical functionalization of BNNT materials and their integration into polycarbonate (PC) matrix. The chemical functionalization is performed through in-situ B-N bond cleavage by bromine treatment in aqueous solution during the removal of elemental boron byproduct contained in the as-produced BNNT material. In addition, the mechanism of the chemical functionalization and the primary results of BNNT-reinforced PC-nanocomposites are discussed.

Keywords: boron nitride nanotube (BNNT), surface functionalization, interfacial compatibility, nanocomposite, polycarbonate (PC)

1 INTRODUCTION

CNTs have become a material of choice for nano-reinforcement since their discovery in the beginning of 1990s [1]. Due to their excellent electrical, thermal and mechanical properties with extremely low density and high aspect ratios, a range of CNT-enhanced products are now commercially available [2]. Owing to massive production and supply, CNTs related commercial activity has grown in several areas: from drinking water purification, printable electronic, textile fabrication to body armor and armor vehicles. Furthermore, the scale of availability and variety of CNTs have significantly advanced academic research from single tube devices, macro-assembly to their nanocomposites, for instance, in polymers [3, 4], metals [5, 6] and ceramics [7]. The results in the literature reports indicated that the CNT-integrated polymer nanocomposites demonstrated promising trends to enhance the performance of the neat matrix thus, yielding significant weight-reduction.

Similarly, BNNTs have gained attention as an alternative nanomaterial, because their structures and mechanical properties are analogous to CNTs. But BNNTs possess additional complimentary properties, including optical transparency to visible light, electrical insulation, higher thermal and chemical stability, neutron absorption capability and piezoelectricity. Therefore, BNNTs have emerged as promising nanomaterials that provides enormous potential in the fields of structural and functional nanocomposites, optically transparent, thermally and scratch-resistant materials, high temperature and strain sensor manufacturing and radiation shieldings. Although BNNTs have been successfully synthesized since 1995 [8] that is only few years after the discovery of CNT. The lack of mass-production technology has hampered advances in all research areas until recently, where plasma-generated high temperature sources [9-11] made it possible to break this technological barrier. This led to several scientific developments in the field [12-24]. However, just like with CNTs, the main issues in the use of BNNTs are dispersion and interfacial adhesion due to strong van der Waals interactions amongst the individual tubes. The most effective method used to resolve these issues is surface functionalization to obtain individuals and/or small bundles of tubes with selected functional groups on the external surfaces. Such covalent functional groups can prevent rebundling and be used as secondary functionalities for further anchoring desired linkers or directly to enhance adhesion at the interface of the polymer matrix. However, the surface chemistry of BNNTs is more challenging than that of CNT because of the different electronic structures and bonding characters [8, 25]. Here, we report the surface chemical functionalization of BNNTs through in-situ B-N bond cleavage by bromine treatment in a aqueous solution with assistance of ultrasonication. The functionalized BNNT materials are further integrated into polycarbonate (PC) matrix for the development towards strong and lightweighting transparent armor and armor vehicle applications.

2 MATERIALS AND PROCESSES

2.1 Synthesis of BNNT Materials

The scalable thermal induction plasma production process developed at the National Research Council Canada (NRC) was used for the manufacture of the highly crystalline, small-diameter (~ 5nm) and few-walled (2-4) BNNT materials. Commercial hexagonal boron nitride (h-BN) powder (99.5%, MK-hBN-N70, M. K. Impex Corp.) was used as the feedstock [9]. Typical visual appearance and microscopic morphology of the as-produced BNNT materials from this process are shown in Figure 1. The major impurities and by-products include non-vaporized h-BN blocks, newly generated h-BN phase such as amorphous BN flakes/particles, organic and/or polymeric BN and B–N-H species and elemental boron particles.

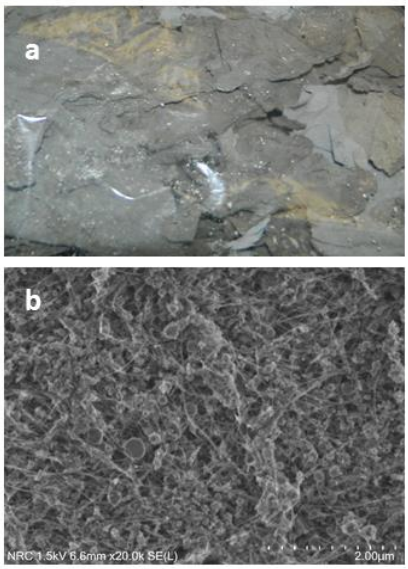

Figure 1: a) Optical image of as-produced BNNTs; b) a representative SEM image of as-produced BNNTs.

2.2 Surface Functionalization of BNNTs

These impurities can heavily interfer with the surface chemistry of BNNT. Thus, they must be removed before undertaking any chemistry on the BNNT. The vast majority of BN-impurities can be washed/separated out as reported in our previous work [13] through a three-stage purification protocol. However, the heavier elemental boron particles and aggregates remain in the sample together with the BNNT material. These boron particles can be removed through the well-known chemical reaction with bromine in aqueous solution forming boric acid as illustrated in equation (1). The resulting boric acid is highly soluble in water and can be fully washed away from the BNNT sample.

$$2B + 3Br_2 \longrightarrow 2BBr_3 \xrightarrow{nH_2O} 2B(OH)_3 + 6HBr \qquad (1)$$

Interestingly, once the available elemental boron particles are fully etched away by bromine, the excess bromine can further attack the B-N bonds in the BNNT network in aqueous solution with the assistance of ultrasonication, resulting in the B-N bond cleavage and forming surface functional OH and NH_2 groups as illustrated in Figure 2.

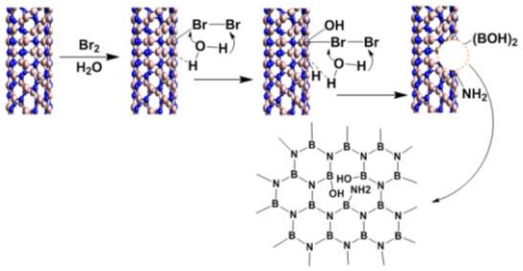

Figure 2: Proposed surface functionalization mechanism through bromine treatment on BNNT tubes [13].

The functionalized BNNTs are soluble in water solution around neutral pH and the solution is stable for a few years. However, the BNNTs in the solution can be precipitated within in a few seconds by adjusting the solution to either basic or acidic conditions as demonstrated in Figure 3. The precipitated BNNT sample has an estimated purity about 80 wt% through SEM analyses.

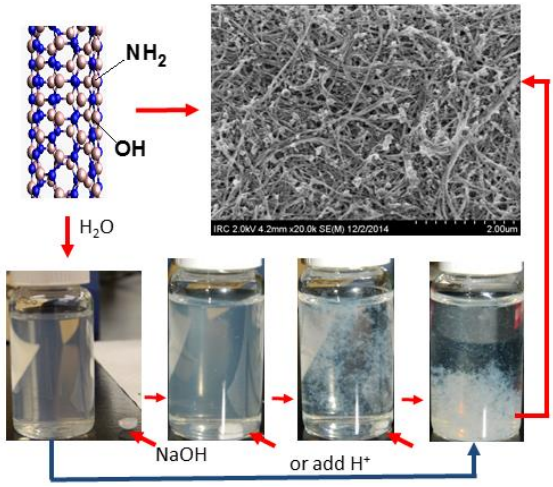

Figure 3: The soluble BNNTs precipitate with changes of the neutral solution to either basic or acidic condition.

2.3 BNNT/PC Nanocomposite Preparation

Commercial polycarbonate Lexan PC Resin 141R-112 was used as the polymer matrix. A typical 4 wt% functionalized BNNT/PC composite sample was prepared as follows: 35 g of PC was dissolved in 450 mL of chloroform, and 1.46 g of functionalized BNNTs was dispersed in 150 mL of DMF with the assistance of bath-ultrasonication. The PC-chloroform solution was then mixed with the BNNT suspension. The mixture was stirred with a magnetic stirring bar overnight at room temperature.

The mixture became a semi-solid gel and was dried in a vacuum oven at 60 ºC. After removal of the major solvents, the solid sample was further dried at 220 ºC. No melting of the sample was observed at such temperature both in vacuum oven and in conventional oven. In comparison, neat PC beads melted together below 200 ºC. For comparison, 1 wt% and 2 wt% of the functionalized BNNT/PC composites were also solvent-processed in the same way as the 4 wt% sample and a neat PC sample as a baseline as well.

The dry BNNT/PC composite samples and the neat PC sample were dried at 120 ºC overnight and then melt-mixed at 250 ºC using a Thermo Haake MiniLab conical twin screw co-rotating extruder. The melting sample was allowed to re-circulate for 3 min within the barrel/screw system by controlling a valve at the end of the screws to allow a better mix of BNNTs before extruding. The extruded sample was pelletized into small pieces that were used for rectangular plaques (25x120x1.2 mm) preparation through compression molding using a Carver hot press. Tensile tests were carried out following ASTM D638 protocol (type IV tensile bar: 25x6 mm) with a load cell of 5 kN and a speed of 5 mm/min at room temperature. The test results were averaged from minimal of four coupons.

3 RESULTS AND DISCUSSION

Like with the CNTs, the main issues in making BNNT composites are dispersion/exfoliation in and adhesion to the matrix. The most effective way to resolve these barriers is to have covalent surface-functionalization [12, 15, 16, 21, 23]. The attached pendants reduce the van der Waals attractions because the tubes cannot get sufficiently close to each other thus promoting and maintaining ex-foliation. Furthermore, covalent functionalization can be used to attach functional groups that promote interactions with the matrix. The reaction of bromine with BNNTs occurred due to the polarity of the B-N bond. Here, bromine binds on B site and cleaves the B-N bond through spontaneous hydrolyzation of the B-Br bond producing OH and NH_2 functional groups as illustrated in Figure 2. The resulting functionalized BNNTs have been characterized with TGA-FTIR showing water and ammonia releases from the samples at 108 ºC and 225 ºC, respectively. Based on the weight loss and assuming the OH and NH_2 funcional groups in the 2:1 ratio as proposed in Figure 2, one can estimate the degree of functionalization as 2 OHs and 1 NH_2 per every 53 BN pairs [13]. The high solubility of the functionalized BNNTs in neutral water as demonstrated in Figure 3 indicated that OH and NH_2 groups have formed hydrogen bond network with water molecules, which stablized the BNNTs in water for a long time period. However, this stability can be interrupted by adjusting the solution pH to either basic or acidic conditions. This is because the partial hydrogen bond network involving either or both OH or/and NH_2 are converted to salts that cause the precipitation of the functionalized BNNTs.

The OH and NH_2 functionalized BNNTs was integrated into PC matrix at the loading of 1, 2 and 4 wt% in a mixture solution of DMF and chloroform, wherein PC is soluble in $CHCl_3$ and BNNTs are well-dispersed in DMF. To further improve the dispersion of BNNTs in the PC matrix, the composite powder was melt-mixed and circulated for additional 3 minutes in the barrel/screw system of the mini-extuder before extruding. The pelletized sample was characterized through their cryo-fractured cross section by SEM and TEM microscopic analyses as shown in Figure 4 as the representative surface morphology and micro-structure views. In the SEM fractures as shown in Figure 4a, a large BNNT bundle aggregate is observed and in other area, some small BNNT bundles are observed. However, uniformly dispersed individual BNNT tubes are observed all over the matrix and aligned with the extrusion direction as shown from the cryo-TEM images of Figure 4b and c. Meanwhile, there are still variant sizes of impurity particles that are distributed within the PC matrix and might have significant negative impact on the mechanical performance.

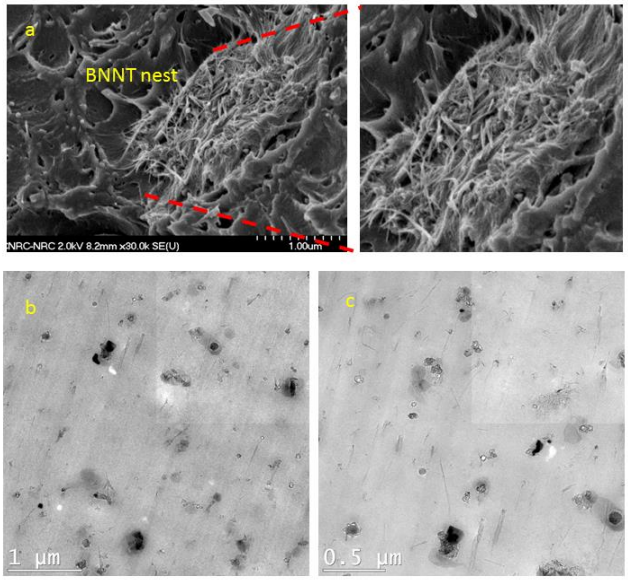

Figure 4: a) SEM image; b) and c) TEM images of cryo-fractured BNNT/PC (4 wt%).

	Young's Modulus (MPa)	Tensile Stress @ Max load (MPa)	Tensile stress @ break (MPa)	Tensile strain @ break (%)
Neat PC	2400±90	67.6±0.6	50.1±2.6	76.2±26.0
1 % BNNT	2430±140	68.2±0.4	55.8±7	101±62
2 % BNNT	2640±207	61.3±8.6	21.9±21.4	9.2±5.2
4 % BNNT	2790±170	52.9±20.5	44.1±11.7	8.7±9.5

Table 1: Comparison of tensile properties of the BNNT/PC composites with neat PC.

The preliminary testing results of BNNT/PC composites and neat PC prepared by melt-mixing process after compression molding are collected in Table 1. The Young's modulus of BNNT/PC composites of 2 and 4 wt% have slightly increases by 9% and 16% with respect to the neat PC, respectively, while their tensile stress at max load decreased correspondingly by 9 and 22%. The 1 wt% sample increased the strength at break by 11% and the elongation at break by 32%, while keeping the same rigidity and strength at yield as the neat PC. The tensile strain at break decreased significantly for the higher BNNT loadings indicating a substantial increase in brittleness. The lack of substantial improvement in the tensile strength or modulus is most probably due to the insufficient dispersion of BNNTs and still weak interaction with the PC matrix as suggested by the SEM and TEM cross section analyses. The large BNNT aggregates and impurity particles could evenatually compromise the reinforcement from the individual dispersed BNNT tubes in the PC matrix.

4 CONCLUSION

This study provided a way to improve the compatibility of BNNT with PC matrix. Here, we used OH and NH_2 functionalization. These functional groups provided marginal improvement in the mechanical performance. The results clearly showed that a better dispersion of BNNTs and more interfacial adhesion are needed.

REFERENCES

[1] S. Iijima, Nature 354, 56, 1991; A. Oberlin, M. Endo, A. T. Koyama, J. Cryst. Grow. 32, 335, 1976.

[2] M. F. L De Volder, S. H. Tawfick, R. H. Baughman, A. J. Hart, Science 339, 535, 2013.

[3] J. Chen, L. Yan, Advances in Materials 6, 129, 2017.

[4] S. H. Park, J. Bae, Recent Pat. Nanotechnol. 11, 109, 2017.

[5] D. Janas, B. Liszka, Mater. Chem. Front. 2, 22, 2018.

[6] S. R. Bakshi, D. Lahiri, A Agarwal, International Materials Reviews, 55, 41, 2010.

[7] J. Cho, A. R. Boccaccini, M. S. P. Shaffer, J. Mater. Sci. 44, 1934, 2009.

[8] N. G. Chopra, R. J. Luyken, K. Cherrey, V. H. Crespi, M. L. Cohen, S. G. Louie, A. Zettl, Science 269, 966, 1995.

[9] K. S. Kim, C. T. Kingston, A. Hrdina, M. B. Jakubinek, J. W. Guan, M. Plunkett, B. Simard, ACS Nano, 8, 6211, 2014.

[10] A. Fathalizadeh, T. Pham, W. Mickelson, A. Zettl, Nano Lett. 14, 4881, 2014.

[11] K. S. Kim, M. J. Kim, C. Park, C. C. Fay, S. H. Chu, C. T. Kingston, B. Simard, Semicond. Sci. Technol. 32, 013003, 2017 and references therein.

[12] J. W. Guan, B. Ashrafi, Y. Martinez, M. B. Jakubinek, M. Rahmat, K. S. Kim, B. Simard, Nanocomposites, 4, 10, 2017.

[13] J. W. Guan, K. S. Kim, M. B. Jakubinek, B. Simard, ChemistrySelect 3, 9308, 2018.

[14] W. Meng, Y. Huang, Y. Fu, Z. Wang, C. Zhi, J. Mater. Chem. C 2, 10049, 2014.

[15] H. Shin, J. W. Guan, M. Z. Zgierski, K. S. Kim, C. T. Kingston, B. Simard, ACS Nano 9, 12573, 2015.

[16] S. Lin, B. Ashrafi, K. Laqua, K. S. Kim, B. Simard, New J. Chem. 41, 7571, 2017.

[17] M. Rahmat, B. Ashrafi, A. Naftel, D. Djokic, Y. Martinez-Rubi, M. B. Jakubinek, B. Simard, ACS Appl. Nano Mater. 1, 2709, 2018.

[18] M. Rahmat, M. B. Jakubinek, Y. Martinez-Rubi, A. Nafterl, B. Ashrafi, B. Simard, Polymer Composites DOI : 10.1002/pc.24995.

[19] K. S. Kim, M. Couillard, H. Shin, M. Plunkett, D. Ruth, C. T. Kingston, B. Siamrd, ACS Nano 12, 884, 2018.

[20] M. B. Jakubinek, A. Ashrafi, Y. Martinez-Rubi, M. Rahmat, M. Yourdkhani, K. S. Kim, K. Laqua, A. Yousefpour, B. Simard, Intern. J. Adhesion and Adhesives 84, 194, 2018.

[21] C. A. de los Reyes, K. L. Walz-Mitra, A. D. Smith, S. Yazdi, A. Loredo, F. J. Frankovsky, E. Ringe, M. Pasquali, A. A. Marti, ACS Appl. Nano Mater. 1, 2421, 2018.

[22] Z. Wang, Q. Li, J. Liu, H. Li, S. Zheng, J. Nanomater. 6727046, 2018.

[23] C. A. de los Reyes, A. D. S. McWilliams, K. Hernandez, K. L. Walz-Mitra, S. Ergulen, M. Pasquali, A. A. Marti, ACS Omega 4, 5098, 2019.

[24] S. Quiles-Díaz, Y. Martínez-Rubí, J. W. Guan, K. S. Kim, M. Couillard, H. J. Salavagione, M. A. Gómez-Fatou, B. Simard, ACS Appl.Nano Mater. 2, 440, 2019.

[25] D. Golberg, Y. Bando, Y. Huang, T. Terao, M. Mitome, C. Tang, C. Zhi, ACS Nano 4, 2979, 2010.